Introduction to plasma

Part 04: Magnetic Reconnection

Magnetic Reconnection

Magnetic reconnection is a phenomenon that is of particular importance in solar system plasmas. In the solar corona, it results in the rapid release to the plasma of energy stored in the large-scale structure of the coronal magnetic field, an effect that is thought to give rise to ***solar flares***. Small-scale reconnection may play a role in heating the corona, and, thereby, driving the outflow of the ***solar wind***. In the Earth's magnetosphere, magnetic reconnection in the magnetotail is thought to be the precursor for ***auroral sub-storms***.

The Induction equation:

Governs the evolution of the magnetic field in a resistive-MHD plasma. The first term on the right-hand side of this equation represents the convection of the magnetic field by the plasma flow. The second term describes the resistive diffusion of the field through the plasma. The relative magnitude of the terms is conventionally measured in terms of ***magnetic Reynolds number*** $\mathbf{R_m}$. When $\mathbf{R_m << 1}$ ($\sigma \to 0$) , the diffusive term overcomes the convective term.

Induction Equation: $\frac{\partial \mathbf{B}}{\partial t} = \nabla \times (\mathbf{V} \times \mathbf{B}) + \frac{1}{\sigma \mu_o} \nabla^2 \mathbf{B} \Rightarrow$

$$\begin{cases} \text{diffusivity: } \eta = \dfrac{1}{\sigma \mu_o} \\ \dfrac{1}{\sigma \mu_o} \nabla^2 \mathbf{B} \sim \dfrac{|\mathbf{B}|}{\sigma \mu_o L^2} \\ \nabla \times (\mathbf{V} \times \mathbf{B}) \sim \dfrac{|\mathbf{V}| \cdot |\mathbf{B}|}{L} \\ \dfrac{\partial \mathbf{B}}{\partial t} \approx \dfrac{\mathbf{B}}{\tau_d} \\ \dfrac{1}{\sigma \mu_o} \nabla^2 \mathbf{B} \approx \dfrac{1}{\sigma \mu_o} \dfrac{\mathbf{B}}{L^2} \end{cases} \Rightarrow \begin{cases} \text{Magnetic Reynolds Number} \\ R_m = L|\mathbf{V}| \sigma \mu_o = \dfrac{L|\mathbf{V}|}{\eta} \\ \text{Lundquist number} \\ S = \dfrac{L|V_A|}{\eta} \\ \text{Dissipation Time Scale} \\ \tau_d = \sigma \mu_o L^2 = \dfrac{L^2}{\eta} \end{cases}$$

The dissipation time scale $\boldsymbol{\tau_d}$ is the time scale for the dissipation of magnetic energy over length scale **L.**

Magnetic Reconnection in Solar and Space Plasmas ???

It turns out that $\mathbf{R_L >> 1}$ values are expected because of the extremely large length scales of solar system plasmas. For instance, $\mathbf{R_L \sim 10^8}$ for solar flares, where as $\mathbf{R_L \sim 10^{11}}$ is appropriate for the solar wind. In calculating $\mathbf{R_L}$, we have identified the length scale **L** with the characteristic size of the plasma under investigation. It seems reasonable to neglect diffusive processes altogether in solar system plasmas. It must be noted, however, that the $\mathbf{R_L >> 1}$ -values upon which the applicability of the ***frozen flux*** constraint was justified were derived using the large overall spatial scales of the systems involved. However, strict application of this constraint to the problem of the interaction of separate plasma systems leads to the inevitable conclusion that **structures will form having small spatial scales**, at least in one dimension: that is, the thin current sheets constituting the cell boundaries. It is certainly not guaranteed, that the effects of diffusion can be neglected in these boundary layers.

The MHD diffusion Equation at a 1-D current sheet

Consider a simple current sheet across which the magnetic field reverses:

$$\mathbf{B}=B(x,t)\mathbf{y} \text{ and } B(x,t=0)=\begin{cases}+B_o, & x>0\\ -B_o, & x<0\end{cases}$$

From the1-D Induction equation (Diffusive term retained):

$$\left.\begin{aligned}\frac{\partial B}{\partial t}&=\eta\frac{\partial^2 B}{\partial x^2}\\ j_z&=\frac{1}{\mu_o}\frac{\partial B}{\partial x}\end{aligned}\right\}\Leftrightarrow\begin{cases}B(x,t)=B_o\,\mathrm{erf}\left(x\sqrt{\dfrac{1}{4\eta t}}\right)\\ \dfrac{\partial j_z}{\partial t}=\eta\dfrac{\partial^2 j_z}{\partial x^2}\\ J=\int_{-\infty}^{\infty}j_z dx=\dfrac{B_o}{\mu_o}\\ \mathrm{erf}(\xi)=\dfrac{2}{\sqrt{\pi}}\int_0^{\xi}e^{-u^2}du\end{cases}$$

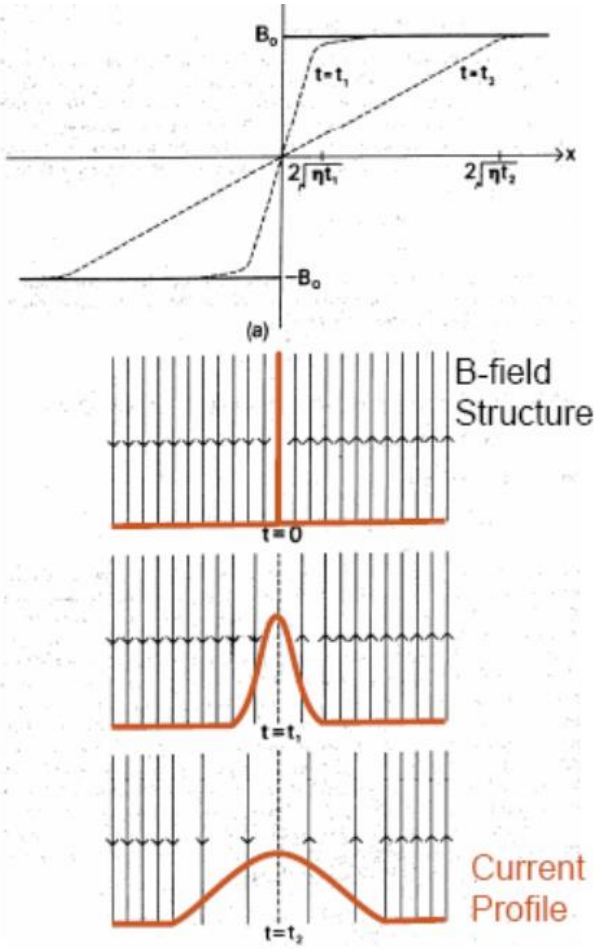

The magnetic field diffuses and annihilates, as illustrated in the figure, the current sheet broadens, the current density **j** weakens but the total current **J** in the sheet remains constant.

Magnetic Reconnection: the Sweet-Parker model (I)

In the Sweet-Parker model the reconnection is the result of an externally imposed flow, or magnetic perturbation. The magnetic and plasma flow fields are illustrated in the Figure. The system is two-dimensional and steady-state with the reconnecting magnetic fields being anti-parallel, and of equal strength. At the boundary between the two fields, where the direction of **B** suddenly changes a current sheet of width **l** and length **L>> l** is formed. Plasma is assumed to diffuse into the current layer, along its whole length, at some relatively small inflow velocity $\mathbf{v_{in}}$; is accelerated along the layer, and eventually expelled from its two ends at some relatively large outflow velocity $\mathbf{v_o}$. We have:

Poynting: $|\mathbf{P}| = \left|\frac{\mathbf{E}\times\mathbf{B_i}}{\mu_o}\right| \approx \frac{E\cdot B_i}{\mu_o}$

Ohm far from the Current Sheet

$|\mathbf{E}| = |\mathbf{v_{in}}\times\mathbf{B_i}| \approx v_{in}\cdot B_i$

$|\mathbf{P}| = \delta W = \frac{1}{2}(\rho_m\cdot v_{in})(v_o^2 - v_{in}^2)$

$\Rightarrow$

$$\begin{cases} |\mathbf{P}| \approx \dfrac{v_{in}\cdot B_i^2}{\mu_o} \approx \dfrac{1}{2}(\rho_m\cdot v_{in})v_o^2 \\ \dfrac{1}{2}\rho_m v_o^2 \approx \dfrac{B_i^2}{\mu_o} \end{cases}$$

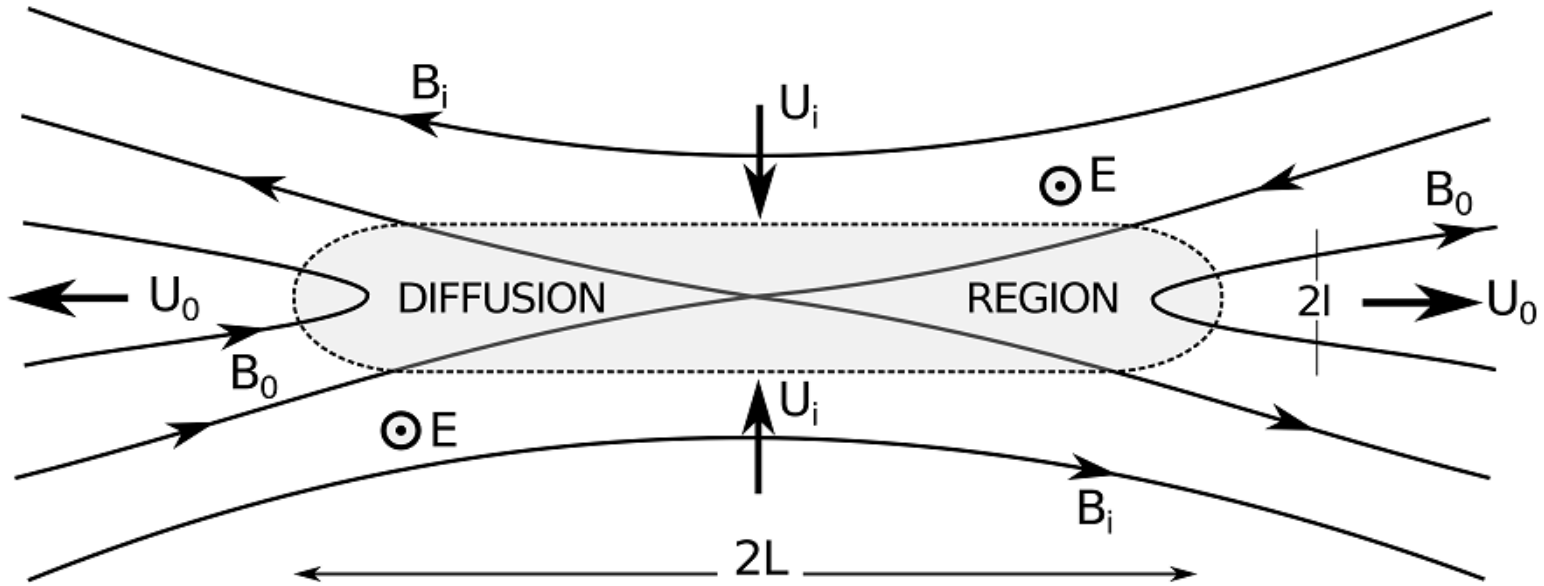

Magnetic Reconnection: the Sweet-Parker model (II)

Continuing from the previous slide:

$$\left.\begin{aligned} |\mathbf{P}| &\approx \frac{v_{in}\cdot B_i^2}{\mu_o} \approx \frac{1}{2}\left(\rho_m \cdot v_{in}\right)v_o^2 \\ \frac{1}{2}\rho_m v_o^2 &\approx \frac{B_i^2}{\mu_o} \end{aligned}\right\} \Rightarrow \begin{cases} v_o = V_A\sqrt{2} \\ V_A = \dfrac{B_i}{\sqrt{\rho_m \mu_o}} \end{cases}$$

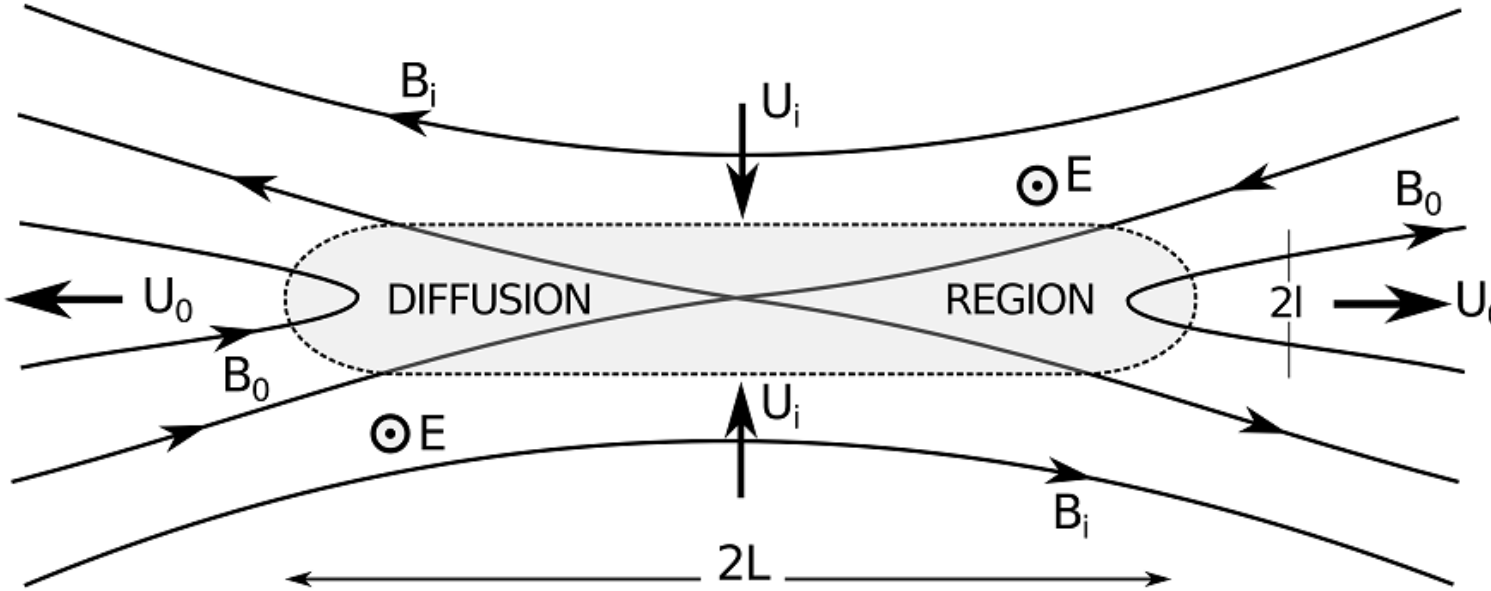

Ohm far from the Current Sheet

$$|\mathbf{E}| = |\mathbf{v_{in}} \times \mathbf{B_i}| \approx v_{in}\cdot B_i$$

Ohm at the Current Sheet+Ampere

$$|\mathbf{E}| = \left|\frac{j}{\sigma}\right| = \frac{B_i}{l\sigma\mu_o}$$

Continuity: $Lv_{in} \approx l\cdot v_o = l\cdot V_A\sqrt{2}$

$$\Rightarrow \begin{cases} v_{in}B_i \approx |\mathbf{E}| \approx \dfrac{B_i}{l\sigma\mu_o} \Rightarrow l = \dfrac{1}{v_{in}\sigma\mu_o} \\ Lv_{in} \approx \dfrac{1}{v_{in}\sigma\mu_o}\left(l\cdot V_A\sqrt{2}\right) \end{cases}$$

Magnetic Reconnection: the Sweet-Parker model (III)

Continuing from the previous slide:

$$\left.\begin{aligned} v_{in}B_i \approx |\mathbf{E}| \approx \frac{B_i}{l\sigma\mu_o} \Rightarrow l = \frac{1}{v_{in}\sigma\mu_o} \\ Lv_{in} \approx \frac{1}{v_{in}\sigma\mu_o} V_A\sqrt{2} \\ V_A = \frac{B_i}{\sqrt{\rho_m\mu_o}} \end{aligned}\right\} \Rightarrow \begin{cases} v_{in}^2 = \dfrac{V_A\sqrt{2}}{\sigma\mu_o L} \Leftrightarrow v_{in} = V_A\sqrt{\dfrac{\sqrt{2}}{\sigma\mu_o L}} \\ v_{in} \approx \dfrac{V_A}{\sqrt{S}} \Leftrightarrow \dfrac{v_{in}}{V_A} = \dfrac{1}{\sqrt{S}} \end{cases}$$

Energy dissipation rate:

Energy density of B × Volume Entering the Current Sheet/Time

$$\frac{dE_{dis}}{dt} = \frac{B^2}{\mu_o}\frac{dV}{dt} \approx \frac{B^2}{\mu_o} L^2 v_{in} \approx\approx \frac{B^2}{\mu_o} \cdot \frac{L^2 V_A}{\sqrt{S}}$$

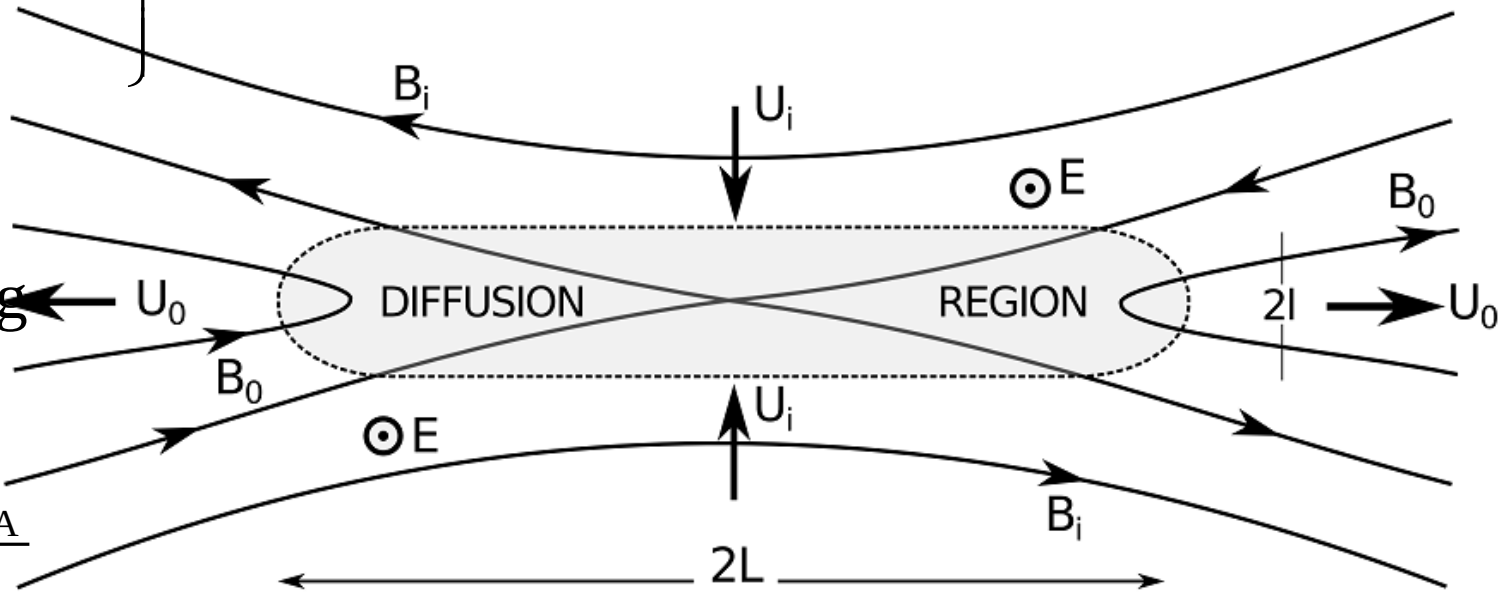

Magnetic Reconnection: the Sweet-Parker model (IV)

Comments on the Sweet-Parker model:

The Sweet-Parker reconnection model is undoubtedly correct. It has been simulated numerically many times, and was confirmed experimentally. The problem is that Sweet-Parker reconnection takes place far too slowly to account for many reconnection processes that are thought to take place in the solar system.

For typical coronal conditions (with a large Lundquist number of $\mathbf{S} \approx 10^{8}-10^{12}$) the reconnection rate is typically $\approx 10^{-4}-10^{-6}$, which yields inflow speeds in the order of $\mathbf{v_{in}} \approx 1000$ km s^{-1} $\times 10^{-5} \approx 0.01$ km s^{-1} and yields extremely thin current sheets with a thickness of $\mathbf{l} = \mathbf{L}(\mathbf{v_{in}}/\mathbf{V_A}) \approx \mathbf{L} \times 10^{-5}$. Therefore, a current sheet with a length of $\mathbf{L} \approx 1000$ km would have a thickness of only $\mathbf{l} \approx 10$ m. So the Sweet−Parker reconnection rate is much too slow to explain the magnetic dissipation in solar flare events.

Hence: We need smaller current sheet size $\mathbf{L}$ (some sort of fragmentation might be proven useful) or higher resistivity $\boldsymbol{\eta}$ (or Both !!!!).

Magnetic Reconnection: the Petschek model (I)

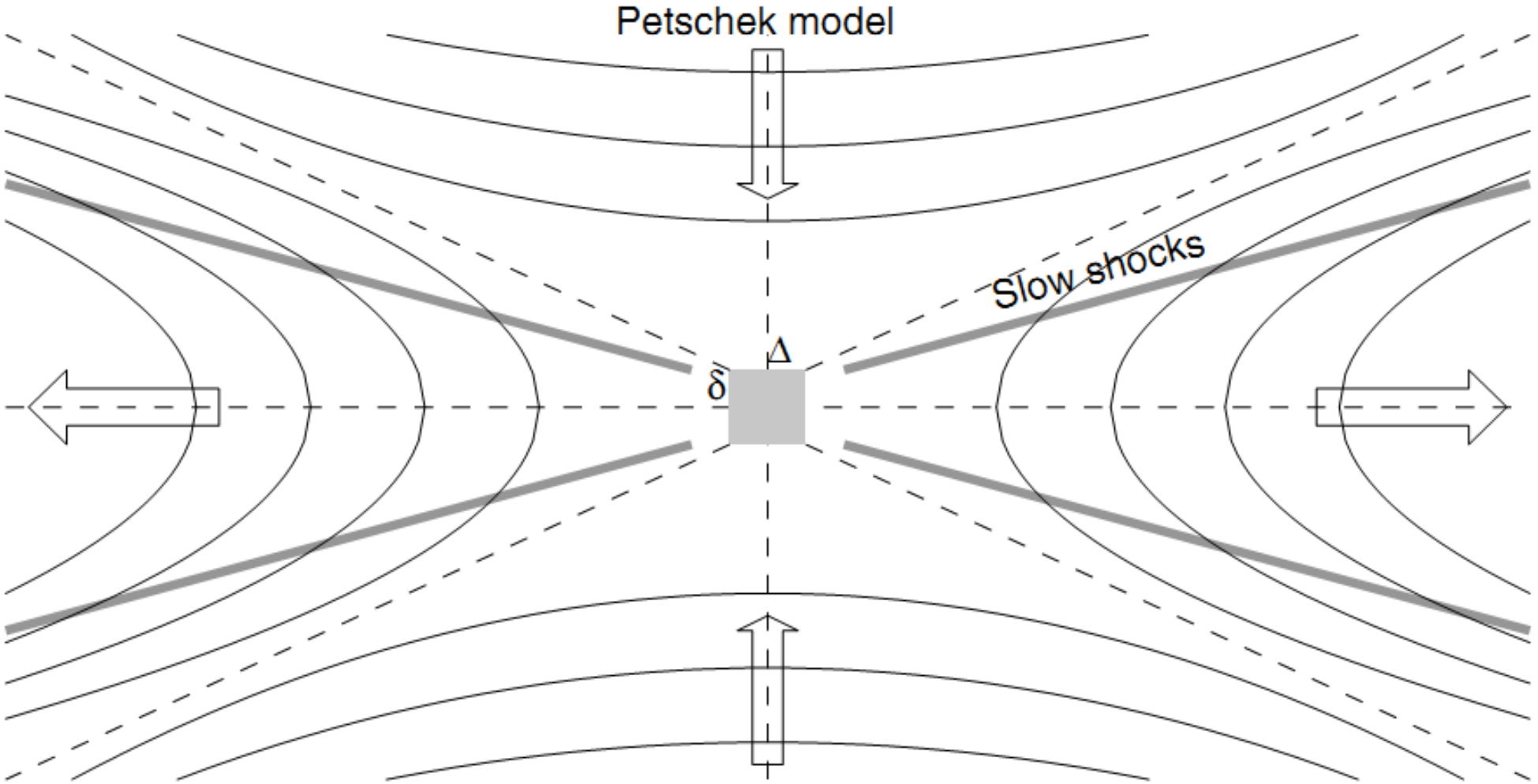

Geometry of the Petschek reconnection model. The geometry of the diffusion region (grey box) is a compact current sheet (≈ **δ**) in the Petschek model; it also considers MHD shocks in the outflow region.

Magnetic Reconnection: the Petschek model (II)

A much faster reconnection model was proposed by Petschek (1964), which involved **reducing the size** of the diffusion region to a very compact area ($\Delta \approx \delta$) that is much shorter than the Sweet−Parker current sheet ($\Delta >> \delta$).
Because the length of the current sheet is much shorter, the propagation time through the diffusion region is shorter and the reconnection process becomes faster. However, in a given external area comparable with the length of the Sweet−Parker current sheet, a much smaller fraction of the plasma flows through the Petschek diffusion region with, where finite resistivity **σ** exists and field lines reconnect.
Most of the inflowing plasma turns around outside the small diffusion region and shocks arise that represent an **obstacle** in the flow and thus are the **main sites where inflowing magnetic energy** is **converted into heat and kinetic energy**.
The **reconnection rate** was estimated $\approx \pi/8\ln(S)$

Tearing-Mode Instability and Magnetic Island Formation

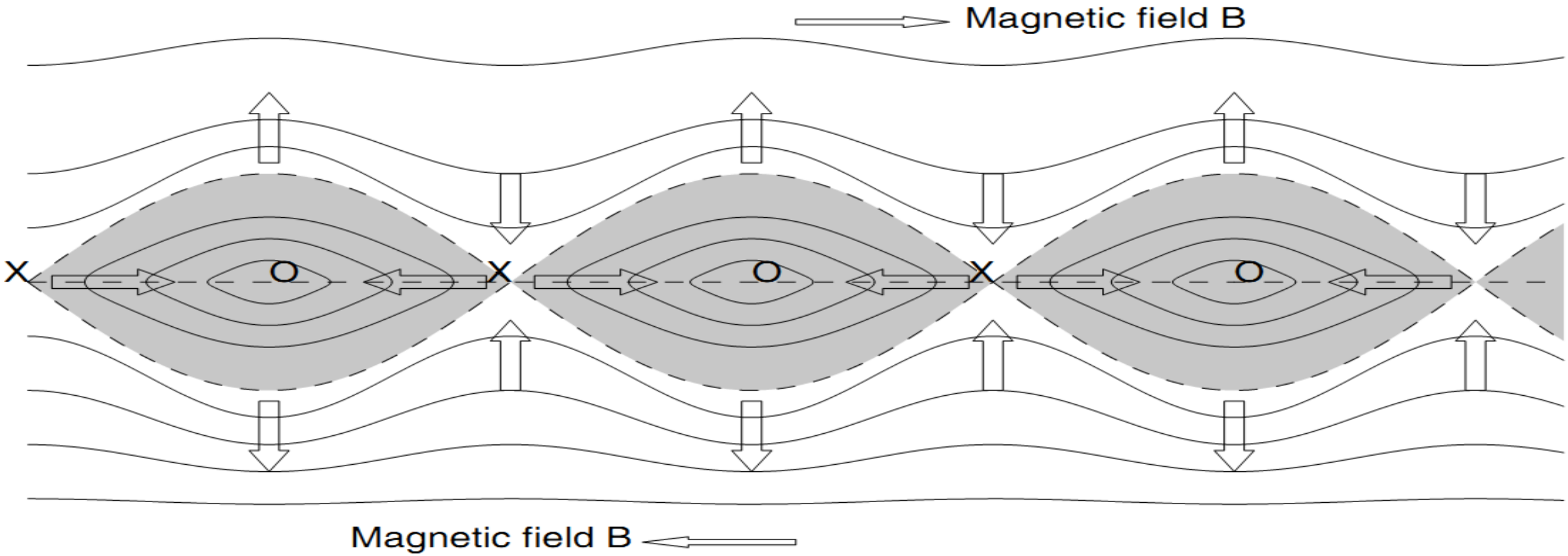

Magnetic island formation by **tearing-mode instability** in the magnetic reconnection region. Magnetically neutral X and O points are formed at the boundary between regions of an oppositely directed magnetic field, with plasma flow in the directions indicated by the arrows. Tearing mode produces magnetic islands in 2D

Coalescence Instabilitv

While tearing mode leads to filamentation of the current sheet, the resulting filaments are not stable in a dynamic environment. If two neighboring filaments approach each other they may enter the **coalescence instability**, which merges the two magnetic islands into a single one. Coalescence instability completes the collapse in sections of the current sheet, initiated by tearing-mode instability, and thus releases the main part of the free energy in the current sheet

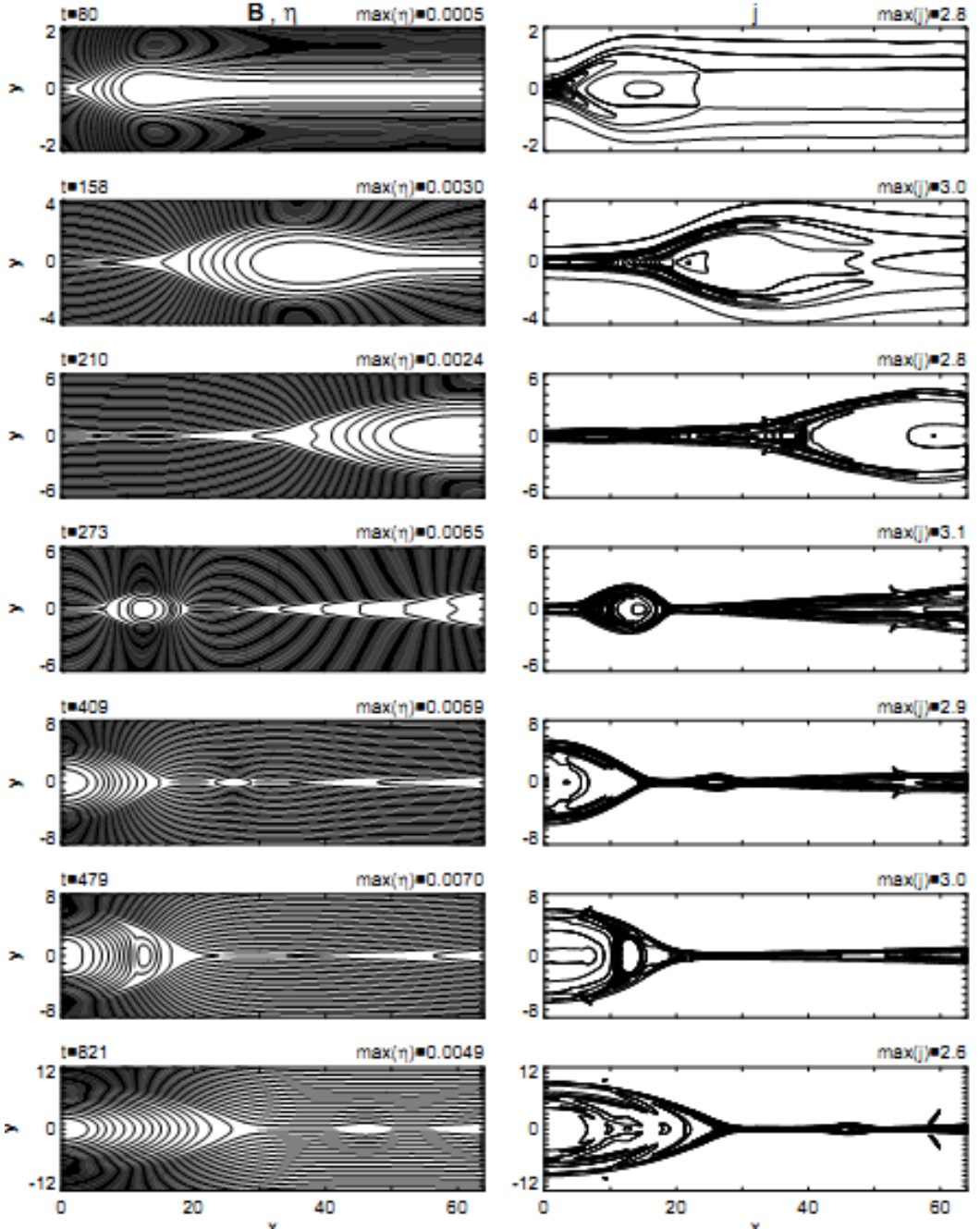

Figure: Magnetic field (left panels) and current density (right panels) at characteristic times of the evolution. The regions, where anomalous resistivity is excited, are shown shaded in the magnetic field plots

Some 3D Magnetic Reconnection Topologies

Classification of X-type magnetic reconnection topologies: (1) **bipolar** reconnection between two open field lines; (2) **tripolar** reconnection between an open and a closed field line; and (3) **quadrupolar** reconnection between two closed field lines. Pre reconnection field lines are rendered in light grey and at the time of reconnection with dotted lines, while the post reconnection field lines, are in dark grey. 2D versions, invariant in the third dimension (forming arcades) are shown in the upper row, 3D versions in the lower row. Pre reconnection field lines are located behind each other in the 3D versions, but approach each other in the image plane during reconnection. Note that the number of neutral lines (marked with **N**, perpendicular to the image plane) is different in the corresponding 2D and 3D cases

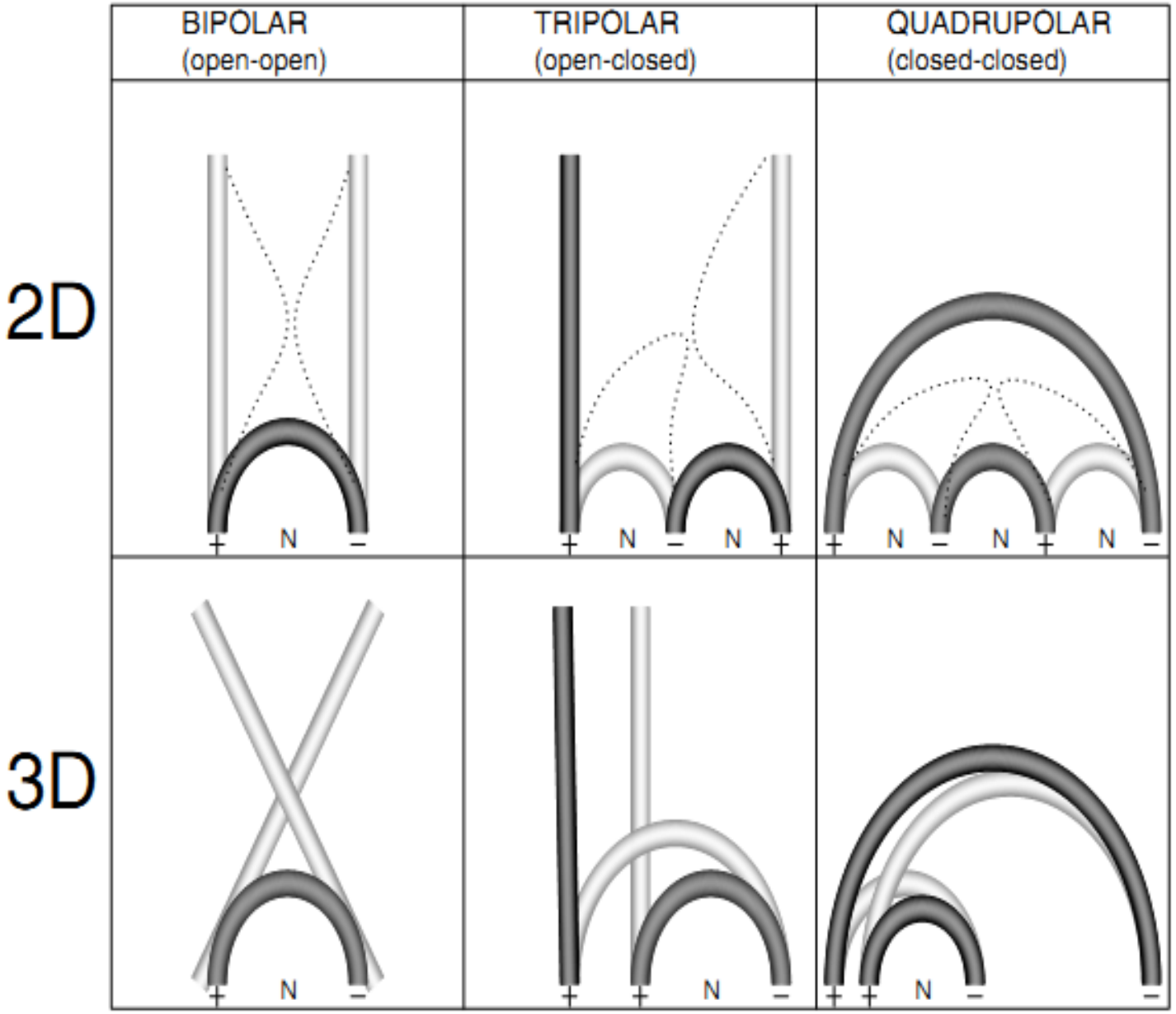

2D vs. 3D Magnetic Reconnection Topologies

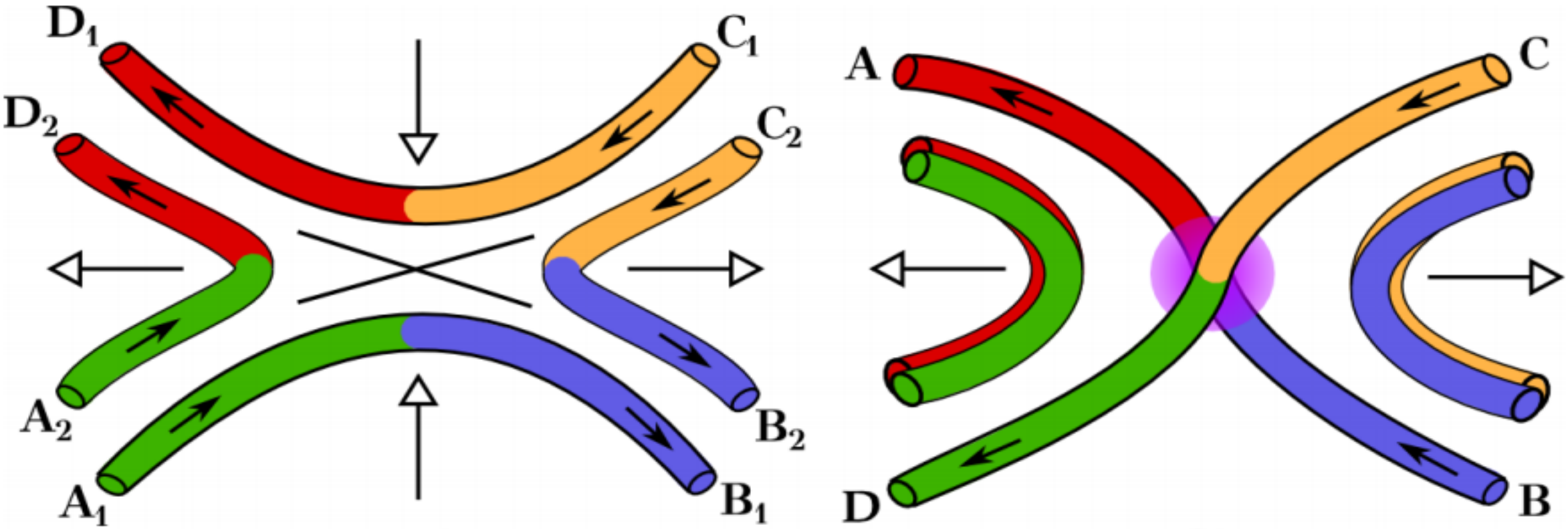

Details of X-type magnetic reconnection topologies: **2D** (left) and **3D** (right).

Topology of 3D Null Points

- **Dipolar domains**: Wherever multiple magnetic dipoles occur, each one defines a domain that contains a volume of magnetic field lines with the same connectivity of positive to negative foot points.
- **Separatrix surfaces**: Different dipolar domains are separated by separatrix surfaces in 3D space.

- **Separators**: Intersections of 2D separatrix surfaces form 1D separator (A separator connects two null points).

- **Null points**: Intersections of 1D separators form 3D null points.

Topology of 3D Null Points

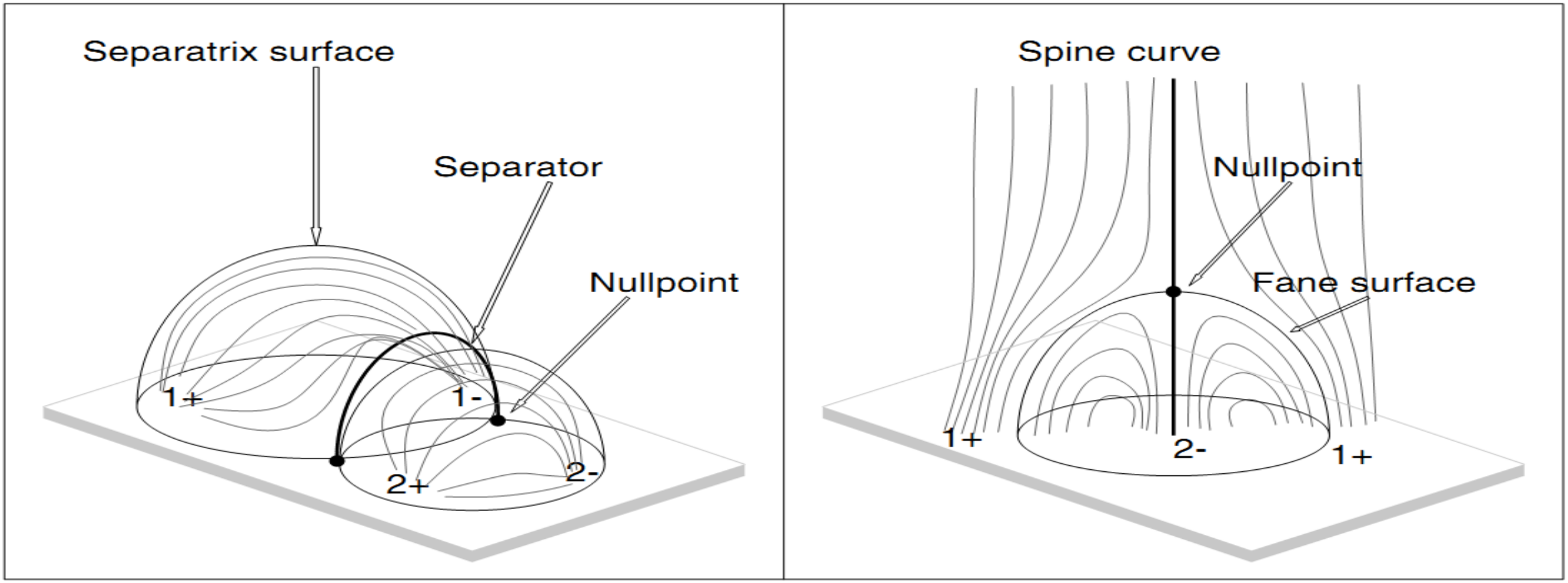

Topology of 3D features for a **quadrupolar** (left) and a **parasitic** region (right). In the quadrupolar region, a new **emerging dipole** (**2+**, **2−**) joins a pre-existing, **older dipole** region (**1+** , **1−**), which are separated by a **separatrix surface**. The intersection of the two separatrix surfaces intersects at the **separator** line, which intersects with the photospheric surface at **magnetic null points**. In the parasitic region (right) a unipolar flux **region 2−** emerges in the center of a pre-existing open field region with polarity 1+. The new regions is shielded from the pre-existing open field by a dome-like fan surface, where the symmetry axis is called the spine, containing a null point at the intersection with the fan dome.